Available online at www.sciencedirect.com
ScienceDirect
C. R. Physique 10 (2009) 13–21
COMPTES RENDUS PHYSIQUE

New approaches in Electromagnetic Compatibility / Nouvelles approches en Compatibilité Electromagnétique

Real-time 3D electromagnetic field measurement instrument with direct visualization

Jean Rioult, Marc Heddebaut *, Divitha Seetharamdoo, Virginie Deniau

French National Institute for Transport and Safety Research (INRETS), LEOST, 20, rue Elisée-Reclus, BP 317, 59666 Villeneuve d'Ascq cedex, France

Available online 17 March 2009

Abstract

Nowadays, a wide variety of terminals are proposed to nomadic users. Generally these terminals provide wireless communication operating at frequencies between one and a few GHz. For technical reasons, including multiple access to the communication channel and battery autonomy, these terminals transmit only during very short periods i.e. transmission bursts. For a direct observation of certain characteristics of the transmitted signals radiated by such terminals, only a few measurement setups exist. This article proposes such a novel real-time 3D electromagnetic field measurement instrument with direct visualization. The prototype used for validation is based on an array of probes regularly attached on a non-conductive rigid loop which is put into fast rotation around the terminal under test. ***To cite this article: J. Rioult et al., C. R. Physique 10 (2009).***

Résumé

Instrument de mesure à visualisation directe en 3D et temps réel du champ électromagnétique. De nombreux terminaux sont actuellement proposés aux usagers nomades. Ces équipements sont souvent dotés d'une capacité de communication sans fil fonctionnant entre un et quelques GHz. Pour des raisons techniques, dont l'accès multiple au canal de transmission et l'autonomie des batteries embarquées, ces terminaux n'émettent que de brèves fractions du temps, sous la forme de salves d'émission. Afin d'observer directement certaines caractéristiques des signaux rayonnés par ces équipements, peu d'appareillages de mesure s'avèrent disponibles. Cet article décrit un nouveau système de visualisation temps réel du champ électromagnétique émis. Le prototype de validation utilise un réseau de sondes maintenues régulièrement espacées sur une boucle isolante mise en rotation rapide autour de l'équipement sous test. ***Pour citer cet article : J. Rioult et al., C. R. Physique 10 (2009).***

Keywords: Antenna radiation pattern; Electromagnetic compatibility; Electric field measurement; Transient radiation; Electronic equipment testing; Probe

Mots-clés : Diagramme de rayonnement d'antennes ; Compatibilité électromagnétique ; Mesure de champ électrique ; Rayonnement transitoire ; Equipement de mesure ; Sonde

* Corresponding author.
E-mail address: marc.heddebaut@inrets.fr (M. Heddebaut).

1631-0705/$ – see front matter
doi:10.1016/j.crhy.2008.12.006

1. Introduction

The experimental methods commonly used to measure the radiated electromagnetic field by a device under test (DUT) consist, up to now, in the use of a single calibrated electromagnetic field sensor. This sensor is mechanically moved step by step on the surface of a defined volume around the DUT. These step-by-step measurements require a long acquisition time and an appropriate post-processing to access to the complete set of results [1].

For acquisition time reduction, multi-sensor techniques are considered [2–4]. A network of sensors is used; the measurement result of each sensor is retrieved, either sequentially using a multiplexer, or through the use of a modulated scattering technique. These measurement techniques are based on vector quantities thus allowing a near-field to far-field transformation [5]. On multi-sensor measurement instruments, sensors are often positioned on a ring or on an arc; the DUT is placed at the ring centre and is rotated around the ring axis [6,7].

The increasing industrial and academic interest in these multi-sensor techniques suggests that the multi-sensor technique will eventually replace the mono-sensor one. Although these techniques improve the data acquisition time, real-time 3D measurements are not really provided.

Nowadays, mobile terminals are more and more miniaturised with electrically small embedded antennas, which unlike large antennas need a thorough characterisation of their radiation properties. Indeed the coupling of the small antenna to the whole system is so significant that the whole terminal has to be characterised while in use. These radiation characteristics are valuable for drawing system design rules, for assessing electromagnetic compatibility compliance as well as overall level of performance.

These mobile terminals generally offer wireless communication capacity within the frequency band starting from 1 GHz to a few GHz for systems such as Global System for Mobile Communications (GSM), Universal Mobile Telecommunications System (UMTS), Bluetooth™, Wireless Fidelity (Wi-Fi) and Ultra-Wide Band (UWB). For technical reasons, including multiple access to the communication channel and battery autonomy, these terminals emit signals only during the short duration of a time-slot. Typical time slot durations are 577 μs for GSM and 625 μs for Bluetooth™ [8].

To measure the radiation characteristics of such a terminal, either the terminal has to function in a steady continuous wave (CW) regime to account for the measurement acquisition time, or a RF signal has to be supplied to the DUT via an external source. However the power amplifiers of the terminal are generally not designed to operate in CW regime; the first solution thus becomes difficult to implement due to power management and excessive heat dissipation. The second solution is an inconvenient one since it is difficult to carry out and intrusive.

For terminals emitting during a short duration, existing measurement setups allowing the characterisation of radiating elements in true real time are not available [9]. This constitutes the motivation of the research work described in this article. The originality lies in the use of a direct 3D visualisation system converting the electric signals generated from an array of radiofrequency probes into a set of different corresponding visible colours radiated by a light emitted diode (LED) piggyback on each probe. Then, each probe is attached at regular intervals on a non-conductive rigid loop put into fast rotation around the terminal under test, thus creating a time sweep, in the same way as an oscilloscope. This time sweep or rotation speed is selected in accordance with the human retinal persistence time and the typical time slot durations of the wireless communication protocols to be evaluated. The prototype described in this communication fulfils these characteristics.

This article is organised as follows. In Section 2, the basic principles of the measurement setup are described. The electronic implementation of an elementary sensor constituting the measurement instrument, as well as a description of our laboratory prototype are further detailed in Section 3. A validation procedure is then proposed. The prototype settings retained are described in Section 4, the calibration procedure in Section 5. Finally, measurement results for a Bluetooth™ wireless communication terminal and then a GSM cellular phone terminal are presented and interpreted in Section 6. In Section 7, conclusions are drawn and directions for future work are given.

2. Measurement principles

The measuring instrument prototype consists in a network of identical sensors fixed along a dielectric loop, at regular intervals. The DUT is placed at the centre of the loop. This loop also contains transmission lines for the sensor feeding and control systems. The role of each sensor is to convert the component of the electromagnetic energy radiated by the EUT and received by the detecting system through the antenna into a corresponding colour shade. The

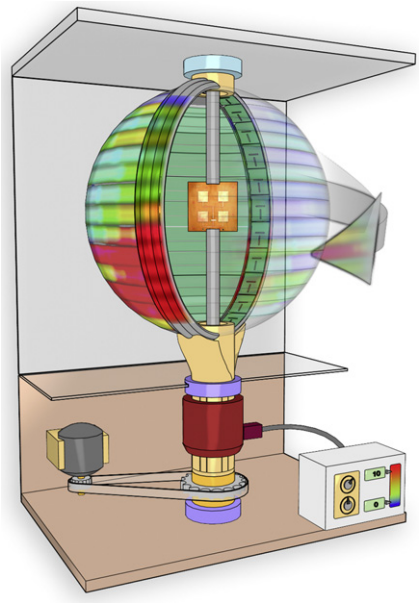

Fig. 1. Schematic representation of the measurement instrument.

Fig. 1. Représentation schématique de l'instrument de mesure.

latter is displayed on the sensor-borne screen; the different colours range from red to green to blue thus representing, by the RGB convention, a variation from a maximum to a minimum level of received energy. The maximum power level corresponding to the darkest red shade displayed as well as the input signal dynamic range given by the different colours can be continuously adjusted. The global brightness of the red, green and blue light-emitting diodes is set almost constant. At constant brightness, using a mix of these primary colours, a very large number of resulting colours can be emitted. In the prototype instrument, 10 colour levels are functional using a commercial off-the-shelf integrated polarisation control circuit.

The loop containing the sensors is rotated up to a rotation speed which allows the visualisation of a complete and continuous measurement sphere thanks to the human retinal persistence of vision. For such a loop, if considered as two semi-annular parts, a rotational speed of 10 to 15 turns per second proves to be sufficient to represent the virtual sphere observed. Fig. 1 depicts a schematic diagram of the measuring instrument prototype implemented at INRETS.

In this example, the DUT is a network of four patch antennas. The rotating collector placed at the foot of the loop supplies the sensors with power and control signals then transmitted to each sensor by the loop-integrated transmission lines.

At a rotational speed of 15 revolutions/s, the response time of the electronic parts of the sensor is much lower than the 66 ms required for a complete turn around the DUT. A large number of successive colour states can then be displayed during one complete turn. An effective transposition between the different signal levels received by the sensor during rotation and the colour shades displayed all around the DUT is thus possible.

The optical emission part of the display screen is coated with a diffusing material layer to avoid the observation of a succession of bright spots. In this given configuration, the network of sensors provides the required global visualisation sphere.

Since each thus-coated sensor does not exactly measure the energy sensed by a discrete element at a given point but rather maps an integration of the radiated energy on a given surface, the diffusing layer has also the role to represent this given equivalent receiving area.

3. Electronic implementation of the unit sensor

Each sensor consists of three main blocks. The first is composed of the radiofrequency (RF) components namely, the antenna to sense the different components of the electromagnetic field and a series of wide-band logarithmic

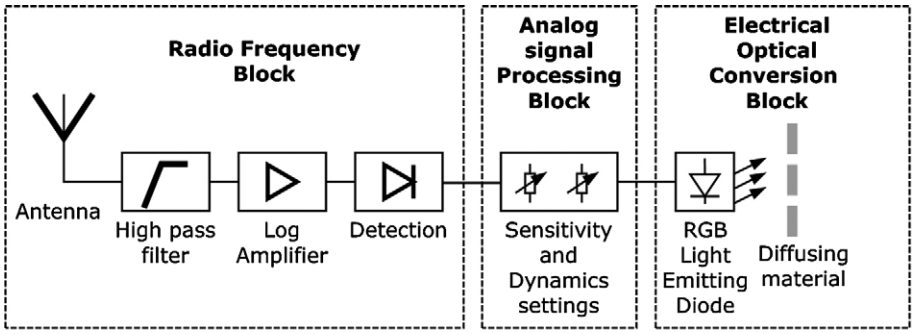

Fig. 2. Synoptic schema of a sensor.

Fig. 2. Schéma synoptique d'un capteur élémentaire.

amplifiers. A low-noise RF amplifier as well as a band-pass filter function can be added just after the antenna or in the antenna. This RF system is followed by a detector. The second block consists in the base-band, low frequency electronic components; it converts the output voltage from the detector into voltage control for the light-emitting diodes. Pre-polarisation control circuits are also integrated in this block; these circuits allow adjusting the measurement dynamic range as well as the maximum power level to the darkest red shade generated. The third block consists mainly of the optical display components as well as the diffusing material layer. Fig. 2 shows the block diagram of an elementary unit sensor.

Practically, each sensor is made up of a three-layer stack: the first layer, closest to and facing the DUT, consists in a microstrip implementation sensor antenna. The second one integrates the RF and base-band electronic chips and circuits. The third layer consists in the coated optical display unit.

In order to realise a first operational prototype, the antenna we have chosen to integrate in the sensor is a slot antenna with a half-wave magnetic resonance at 3.5 GHz. It offers an effective high pass filtering effect reducing low frequency coupling. Each feeding point of the slot antenna on the first layer is connected to the RF and base-band electronic chips and circuits second layer through a soldered transmission line of 6–8 mm. This antenna is separately characterised in an anechoic chamber between 700 MHz and 3 GHz. The antenna radiation efficiency and matching depend on frequency. Therefore, the frequency response of the prototype equipment is not flat in all the usable bandwidth but could be considered reasonably flat for a given limited bandwidth signals delivered by the mobile terminals (GSM phones, Wi-Fi devices, ...) to be evaluated. In this operating frequency band, the slot antenna can be considered to be an electrically small antenna operating in the radiating near field region. At these frequencies, electromagnetic interference mainly occurs due to the presence of stray electric field lines and the use of a slot antenna is sensible in this prototype. A whole set of as-much-as-possible identical sensors are placed on the dielectric loop. Fig. 3 shows on the left-hand side an overall view of the prototype with the set of sensors on the loop surrounding the antenna under test and, on the right-hand side, a zoom-in depiction of the electronic circuit of a given sensor with deployed RF and base-band electronic layers.

As shown in Fig. 3 (left), sets of sensors on the right-hand and left-hand sides of the loop are placed in staggered rows with the aim of minimising the coupling between the antennas of neighbouring sensors.

The particular configuration of the slot antenna used here essentially accounts for the vertically polarised component of electric field. On a semi-resolution level, vertical and horizontal slots can be used on the left-hand side and right-hand side sensor sets thus allowing a separate measurement of the vertical and horizontal components of the electric field.

4. Prototype settings for measurement

The device operates in a frequency range starting from a few hundred of MHz to a few GHz. It covers the operating frequency range of typical communication standards of mobile terminals (GSM, UMTS, Bluetooth^{TM}, Wi-Fi, ...). In the experimental results presented, 10 colour levels are functional and represent an overall dynamic range with a continuous variation from 5 dB to 60 dB (0.5 dB per colour to 6 dB per colour). In its current version, considering a unity gain antenna, the minimum sensitivity of the device is about -60 dBm. The diameter of the loop is a function

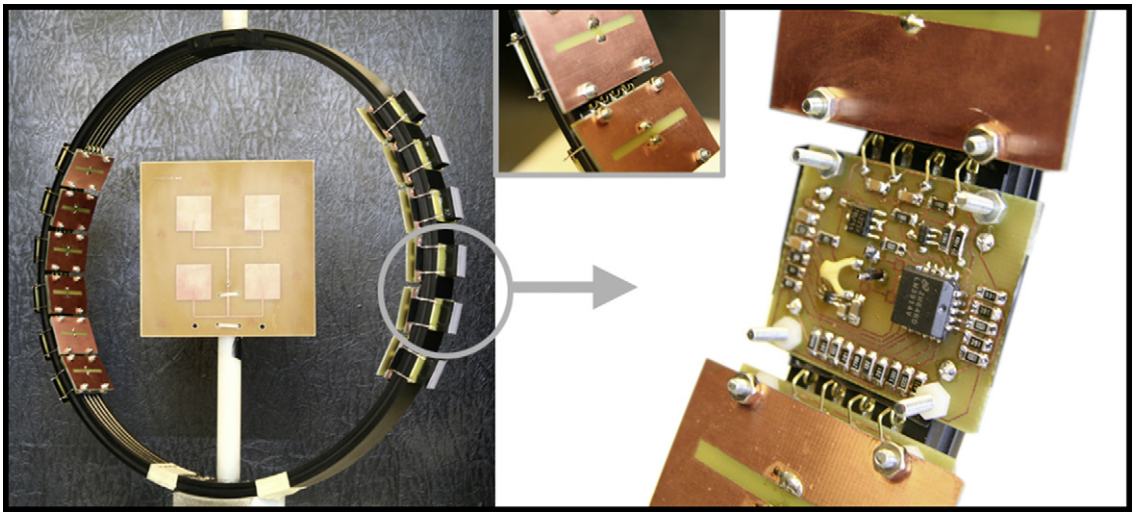

Fig. 3. Overall view of the prototype and a zoom-in depiction of a given sensor.

Fig. 3. Vue générale du prototype et vue détaillée sur un capteur.

of both the operating frequency and the distance required between the DUT and sensing unit. The laboratory-made prototype has a loop diameter of 40 cm.

5. Calibration

The sensor network calibration problem is a particularly difficult one and has not yet been thoroughly dealt with. A first approach to the problem is hereby presented. All of the sixteen sensors constituting the measuring instrument prototype have been realised manually, one by one in the laboratory. As a result, slight differences are very likely. However, the gain of each sensor can be compensated by tuning the pre-polarisation voltage supply of the amplifiers of the circuits. This value is however unchanged within the whole frequency range and cannot compensate for deviations in the frequency response of antennas for instance. A calibration test was carried out by placing the sensor in an anechoic chamber with a mono-chromatic incident wave at 2 GHz. This wave source is placed at a distance of 5 m to the prototype. We assume that the incident field is almost constant in the measurement volume defined by the sphere [10,11]. One would thus expect a uniform field magnitude and the emission of a single colour shade. Fig. 4 shows the result obtained of the measurement configuration described.

The lighter shades (colour changing from blue to green) represent a variation of about 3 dB of the signal measured. Industrially-designed sensors would have allowed the production of sensors with less dispersive performances. However, the calibration of this prototype deserves to be studied more thoroughly with probably an individual calibration process for each sensor [12,13].

6. Measurement results

To validate the prototype, two different types of measurement have been carried out. The first one is a comparative assessment of our measurement configuration by reproducing results which also be provided by conventional and existing measuring instruments [14,15]. The second type of measurement presented is specific to the measuring instrument described in the previous sections with the aim of highlighting the novel measurement possibilities offered by our prototype. The configurations chosen consider the radiation of terminal equipments for different communication protocols during their short transmission times. These measurements were performed using the prototype installed in an anechoic chamber.

6.1. Conventional measurement results

For the comparative assessment with existing conventional measuring instruments, a network of four patch antennas (depicted in Fig. 3) is considered. This antenna is matched at 2.45 GHz and is fed by a continuous wave generator

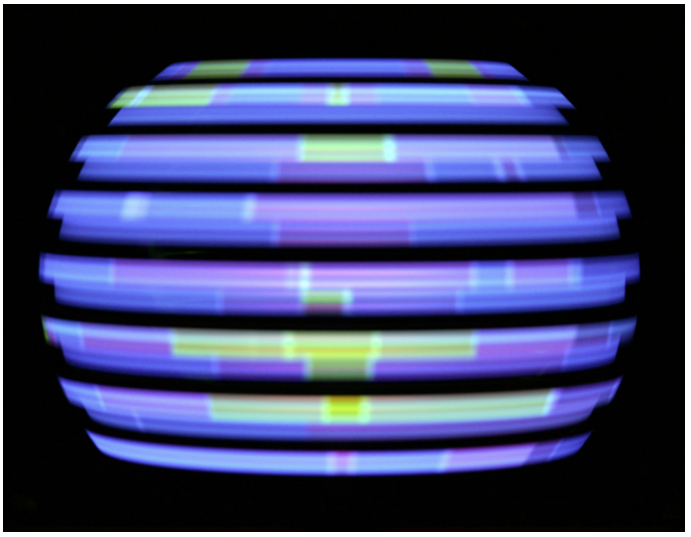

Fig. 4. Global response of the measurement prototype to a far-field source.
Fig. 4. Réponse globale du prototype à une illumination en champ lointain.

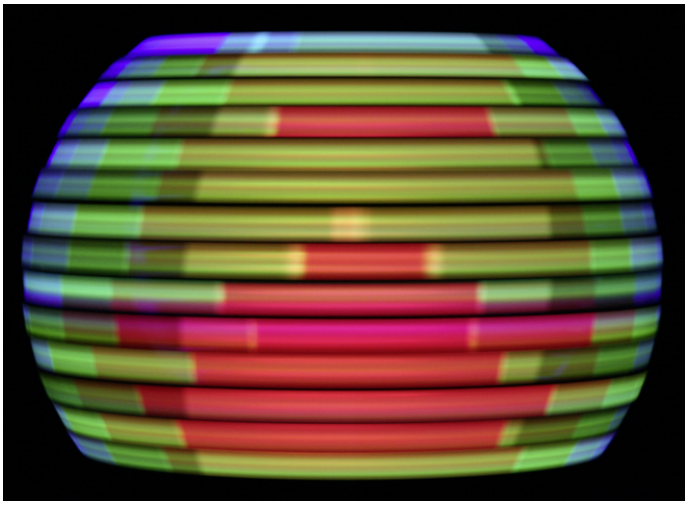

Fig. 5. Antenna radiation pattern visualisation with the prototype.
Fig. 5. Visualisation d'un diagramme de rayonnement à l'aide du prototype.

at 2.45 GHz. The estimated gain of the antenna is 9 dBi. A 0 dBm power level is injected. Fig. 5 shows the front side of the display provided for the antenna under test on. The darkest shades represent the maximum values of electrical energy radiated in these given directions, thus showing the radiation pattern of the antenna. For this measurement, ranging from light blue to dark red, a 30 dB global dynamic measurement is selected and displayed using our 10 colour levels prototype, in 3 dB steps.

6.2. Prototype-specific measurement results

For the prototype-specific measurements, two different communication protocols will be studied, namely GSM and Bluetooth™. First, we consider the radiation emitted by a Bluetooth™ class 2 headset with an RF output power ranging from 0 dBm to around +4 dBm. The headset is placed at the centre of the loop which is then put into rotation. The measurement results are shown in Fig. 6. As stated before, a Bluetooth™ frame lasts 625 μs and note also that a

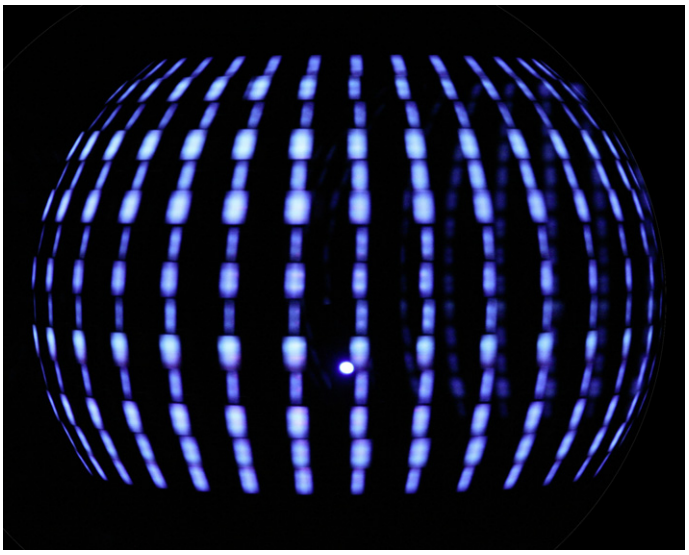

Fig. 6. Direct visualisation of the radiation pattern of a Bluetooth™ headset with the prototype.
Fig. 6. Visualisation directe du rayonnement d'une oreillette Bluetooth™ par le prototype.

Bluetooth piconet can host up to 8 equipments. The radiation emitted by the mobile terminal evaluated during a very short period, in accordance with the Bluetooth™ protocol, is captured and displayed by the measuring instrument. At a speed of 15 revolutions/s, each sensor covers an angular sector area of 1 degree in a period of 185 µs. The illumination of a sensor is therefore maintained for three to four degrees during each emission frame. Because there is only one Bluetooth™ active device in this piconet, other time slots remain unused and dark. Assuming that the calibration step was accurate, for this given DUT, the radiation pattern observed is quasi omni-directional.

Fig. 7(a) presents the measurement results of the configuration consisting in the radiation emitted by a radiotelephone operating under the GSM protocol, at 900 MHz. For this measurement, the door of the anechoic chamber is left open in order to allow a slight coupling of the cellular phone to the outdoor GSM network. At 900 MHz, peak GSM handset power is 33 dBm. A communication is first set up and the phone is then placed in the centre of the loop. Since the mobile phone is only slightly coupled to the GSM fixed network, we assume that full output power is necessary to maintain the communication. In Fig. 7(a), we observe a non-isotropic radiation from this mobile terminal. Fig. 7(b) gives a finer depiction of the output signal from the sensor and illustrates the interpretation of a GSM transmission burst. With a similar analysis as for the Bluetooth headset, a GSM burst can be highlighted with a duration of 577 µs which is given by the optical sensor in terms of a coloured area on a angular sector of a few degrees, followed by a extinction phase of 4.0 ms,characteristic of the GSM protocol.

7. Conclusion

This paper introduces a novel measurement instrument allowing the direct real-time visualisation of 3D electromagnetic radiation of mobile terminals using any single or multiple wireless communication protocols. Using this setup, measurements are performed during the short consecutive emission times associated to these communication protocols.

A prototype has been realised and the implementation of the current version has been thoroughly described. Finally, measurement results are presented for different DUTs, namely a known antenna and two different mobile terminals operating under the Bluetooth™ and GSM protocols respectively. The ability of our measuring instrument prototype to measure the radiation emitted during these short emissions has been demonstrated. Therefore, parameters related to the physical layer of the implemented protocols can be acquired. Although this first prototype is yet to be thoroughly characterised and improved, namely in terms of calibration, the measurements results obtained for mobile terminals constitute a proof-of-concept.

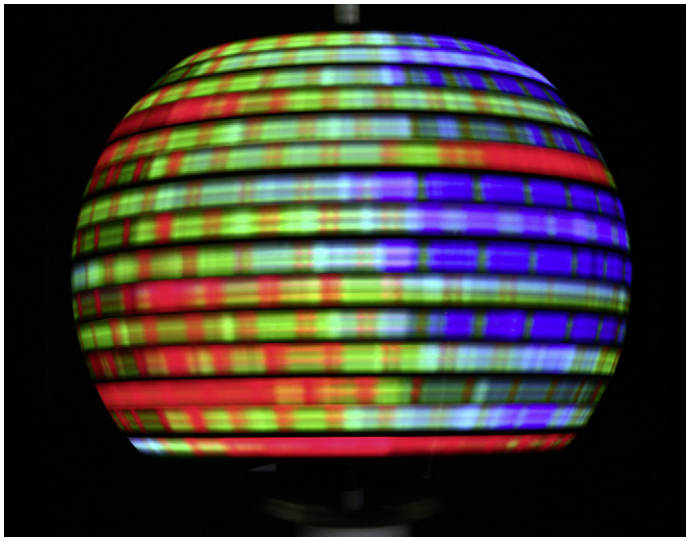

(a)

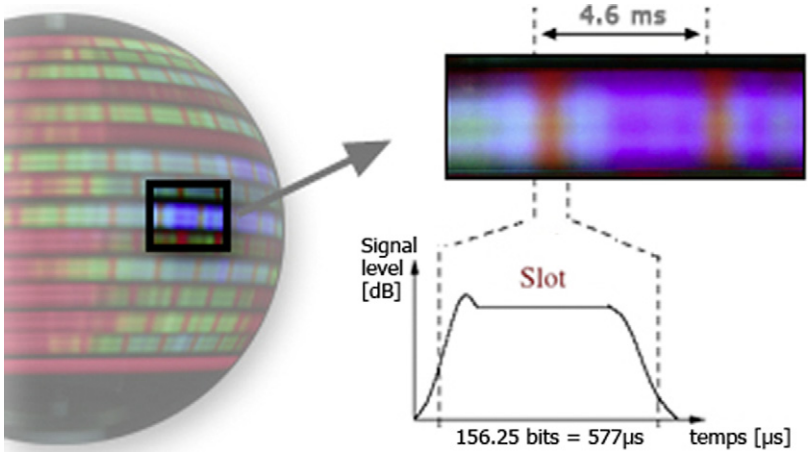

(b)

Fig. 7. (a) Direct visualisation of the radiation pattern of a GSM radiotelephone with the prototype. (b) Detailed analysis of the display and interpretation in terms of the GSM protocol.

Fig. 7. (a) Visualisation directe du rayonnement d'un radiotéléphone GSM par le prototype. (b) Analyse détaillée d'une zone d'affichage et interprétation en termes de protocole GSM.

References

[1] P. Sabouroux, J.M. Geffrin, C. Eyraud, An original microwave near-field/far-field spherical setup: Applications to antennas and scattered field measurements, in: Proceedings of Antenna Measurement Techniques Associate Symposium, Newport, USA, 2005, pp. 292–296.
[2] J.H. Richmond, A modulated scattering technique for the measurement of field distribution, IRE Transactions Microwave Theory Technique 3 (1955) 13.
[3] J.C. Bolomey, et al., Rapid near-field antenna testing via arrays of modulated scattering probes, IEEE Transactions on Antennas and Propagation 36 (1988) 804–814.
[4] Ph. Garreau, K.V. Van't Klooster, J.Ch. Bolomey, D. Picard, Optimization of the arrangement compact range-modulated scattering probe array for rapid far-field antenna measurement, in: Antennas and Propagation, vol. 1, Proceedings 8th International Conference, 1993, p. 376.
[5] J.C. Bolomey, F.E. Gardiol, Engineering Applications of the Modulated Scatterer Technique, Artech House, Dedham, 2001.
[6] P.O. Iversen, P. Garreau, D. Burrell, Real-time spherical near-field handset antenna measurements, IEEE Antennas and Propagation Magazine 43 (2001) 90–94.
[7] C. Qiang, et al., Simultaneous electromagnetic measurement using a parallel modulated probe array, IEEE Transactions on Electromagnetic Compatibility 47 (2007) 263–269.
[8] http://www.bluetooth.com/Bluetooth/Technology/Works/Architecture__Baseband.htm.

[9] R. Azaro, S. Caorsi, M. Pastorino, A 3 GHz microwave imaging system based on a scattering technique and on a modified Born approximation, International Journal of Imaging Systems and Technology 9 (1998) 395–403.
[10] B.K. Chung, H.T. Chuah, Design and construction of a multipurpose wideband anechoic chamber, IEEE Antennas and Propagation Magazine 45 (2003) 41–47.
[11] Ch. Dau-Chyrh, L. Chao-Hsiang, W. Chih-Chun, Compact antenna test range without reflector edge treatment and RF anechoic chamber, IEEE Antennas and Propagation Magazine 46 (2004) 27–37.
[12] M. Whitt, et al., A general polarimetric radar calibration techniques, IEEE Transactions on Antennas and Propagation 39 (1991) 62–67.
[13] K.T. Ng, et al., Amplification and calibration for miniature E-field probes, IEEE Transactions on Instrumentation and Measurement 37 (1988) 434–438.
[14] L.J. Fioged, J. Estrada, P.O. Iversen, Spherical near field testing of small antennas from 800 MHz to 18 GHz, in: IEEE Antennas and Propagation International Symposium, 9–15 June 2007, pp. 2857–2860.
[15] Q. Yuan, et al., Modulated scattering array antennas fort mobile handsets, IEICE Electronics Express 2 (2005) 519–522.